Do Globular Clusters contain Intermediate-Mass Black Holes?

Bobby Hemming

March 2018

Abstract

This work aims to model several different globular clusters, with and without an intermediate-mass Black Hole at the centre, using an N-body simulation. Key features from the cluster evolution are identified. Clusters containing intermediate mass black holes do exhibit different properties than those without, which can be tested against observed data from real clusters. The research has significant limitations due to computational cost of the N-body models and constant timestep used in the leapfrog approximation.

1 Introduction

1.1 Background

Globular Clusters (GCs) are some of the oldest astronomical structures in the Universe, having formed one to two Gyrs after the Big Bang. Research into their evolution can provide an insight into the early Universe. GCs are spherical collections of stars that orbit a galactic core and are tightly bound by gravitational forces. The Milky Way (MW) has around 150 "satellite" GCs that are 10^4 solar masses ($M_\odot$) and orbit the core at radii of up to 40 kiloparsecs (130,000 light-years). GCs are extremely luminous objects, approximately $25,000$ times as luminous as the Sun ($L_\odot$), despite 90% of the mass made up from fainter stars.

The origin of GCs is still poorly understood, but most show stars in the same stage of evolution suggesting they were formed about the same age. As the GCs evolve the stars exchange energy in two-body interactions: stars with low energy are found in the centre of the cluster where they sink to the bottom of the potential well. This is dynamic relaxation also known as core collapse and is caused by gravitational instability in the core [7]. This work will aim to investigate core collapse, as explained in section 1.3. The composition of GCs is mainly of population II star, with a large concentration at the core and fewer further out in a more diffuse halo. GCs contain a low proportion of elements other than hydrogen and helium.

A topical question regarding GCs is whether they contain Intermediate-Mass Black Holes (IMBHs) of masses in the range of 100 to 10^5 $M_\odot$. There is strong evidence for stellar mass black holes 10 to 100 $M_\odot$ and for super-massive black holes (SMBHs) 10^5 to 10^9 $M_\odot$ at galactic cores. In the case of the MW, the SMBH location corresponds to that of Sagittarius A*, a bright radio-source at the centre. There is no conclusive evidence for IMBHs, however it is believed that they could exist at the centre of GCs, but is still a very hypothetical line of research.

Current work investigating Black Holes at the centre of GCs comes from radial velocity measurements of stars orbiting the core to see if they have unusually high velocities. This research aims to probe Globular Cluster collapse and the effect that IMBHs have on the cluster.

1.2 Theory

The most important factor to consider in an astronomical system such as a GC is gravity. Gravitational forces dominate over large distances and are always attractive, so bodies will always accelerate towards each other.

$$\mathbf{F}_i = -G\sum_i^N m_i m_j \frac{\mathbf{r}_i - \mathbf{r}_j}{[|r_i - r_j|^2]^{\frac{3}{2}}} \tag{1}$$

As seen in Eqn.(1), the force on a body, $\mathbf{F}_i$ in a GC depends only on the location of a body relative to all the other bodies. The labels m_i, m_j are the masses of two bodies modelled as point masses, G is the gravitational constant, $|r_i - r_j|$ is the separation of the bodies and $\mathbf{r}_i$, $\mathbf{r}_j$ are the position vectors.

The Virial Theorem states that for a stable, self gravitating, spherical system of equal mass objects; the total kinetic energy is equal to negative one half of the total potential energy [4]. This means for a stable GC (no dynamic relaxation) the total potential and kinetic energy of the GC should follow Eqn.(2),

$$2T + V = 0 \tag{2}$$

where the total kinetic energy is given by T, detailed by Eqn.(3) for a GC and

$$T = \frac{1}{2}\sum_{i=1}^{N} m_i v_i^2 \tag{3}$$

the total potential is given by V, detailed by Eqn.(4) for a GC.

$$V = -\frac{G}{2}\sum_{i=1}^{N}\sum_{j=1}^{N}\frac{m_i m_j}{|r_i - r_j|^2} \tag{4}$$

The labels in Eqn.3 and Eqn.4 are the same as before and with v_i referring to the speed of each particle in the cluster. Both equations sum over all the particles in the cluster to derive the total kinetic and potential energy.

An assumption of the Virial Theorem is that all of the orbits travel on similar orbits of stars are isotropic, that is that they do not have any preferred direction.

The Virial Theorem can be rearranged to give the Virial mass, M_{tot}:

$$M_{tot} \simeq 2\frac{R_{tot}v^2}{G} \quad (5)$$

where the mass has been summed over all the particles to give M_{tot}, R_{tot} is the total radius of the cluster and v is the radial velocity of the cluster which can be found by measuring the velocity dispersion ($v^2 = 3\sigma_D^2$ in three dimensions). By rearranging Eqn.(5) for v and then defining the crossing time, t_{cr}, as the average time taken for a particle to cross over the whole cluster (t_{cr}=$2R/v$) then we have:

$$t_{cr} \approx \frac{1}{\sqrt{G\rho_c}} \quad (6)$$

where ρ_c is the density of the cluster. An interesting point to note is that it is expected, as in a gas, that as a GC evolves it should move to a state of higher entropy. If we take a body in the GC and remove energy from it, it will descend to a lower orbit [5]. The Virial Theorem tells us that the decrease in potential energy is twice as big as the increase in the kinetic energy, therefore we have net removal of energy from the system. Furthermore as energy is removed, but the temperature of the system increases (v has increased), therefore GCs are said to have a negative specific heat. Since GCs have a finite mass, they have a finite escape velocity. So sometimes stars have enough energy to remove themselves from the cluster. The escape velocity required for a star to escape a cluster can be seen if Eqn.5 is rearranged for v.

1.3 Aims

This research aims to investigate the effect of IMBHs on GC evolution. Principally, it will test the quantities described in section 1.2, such as potential and kinetic energy, velocity dispersions and root mean square radii of the cluster of certain GCs; to identify the key differences between a cluster with an IMBH and one without. The aim is to use a computational approach (see Section 3) as the N-body problem is too complex to solve analytically: each body; contribution must be counted as it effects the overall system. Several different spherical GCs will be simulated with different initial conditions (detailed in Section 3.2) for different M_{IMBH}/M_{GC} (IMBH GC mass fractions) and initial concentrations and sizes.

2 Past Work

2.1 History

The first cluster to be observed was Messier 22 (M22), discovered in 1665 by Abraham Isle, a German amateur astronomer. However, because of early telescope's small apertures, stars were not resolved in clusters until Charles Messier observed Messier 4 (M4) in 1764 [5]. Since then, simulating GCs has been an important advance in research in this area as it allows astronomers to follow a GC evolution over millions of years, and for many more stars than is possible observationally or analytically. Important milestones in GC simulations are by Sparzem Aarseth 1996 (10^4 stars), Baumgardt and Makino 2003 (10^5 stars) [2] and Long Wang et al. 2016 (10^6 stars) [3].

2.2 Dr H. Baumgardt

Work by Dr H. Baumgardt is relevant to my work as part of his research concludes the possibility of an IMBH at the centre of Omega Centauri (ω Cen), the largest GC in the MW [2]. Initially Baumgardt sets out to determine the mass to light ratio of GCs by comparing real data collected by Karl Gebhardt et al. for the velocity dispersion and surface brightness profiles of ω Cen against his simulations using the N-body code NBODY6 for clusters with and without IMBHs. The models follow 900 N-body star clusters and varies the initial concentration, size and Black Hole mass. The model also incorporates the effects of stellar evolution and mass segregation. The simulation was run with N = 100,000 stars, IMBH mass ≈ 40,000 $M_\odot$ allowed to evolve for up to 13.5 Gyrs.

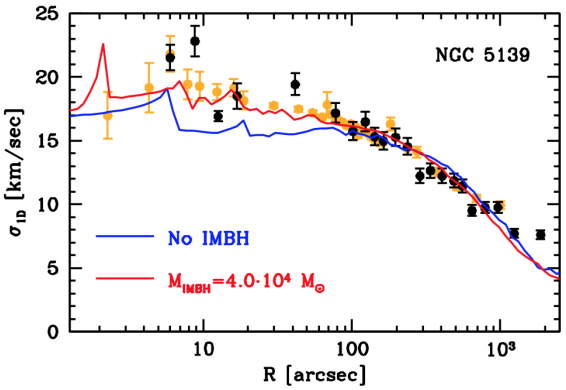

Figure 1. Velocity dispersion profile of ω Cen taken from Fig. 6 of the work by Dr H. Baumgardt [2] which shows the strongest evidence for the presence of an IMBH in a GC. The red line shows the simulation containing an IMBH and the blue line shows the simulation with no IMBH, both are plotted against observed data for the cluster.

It can clearly be seen from Fig.1 that the velocity dispersion profile for ω Cen without a IMBH is in strong disagreement with the observed data. Baumgardt reports a value for $\chi^2 = 2.71$, his second largest disagreement with the observed data. Therefore, his research suggests ω Cen contains an IMBH. This is an interesting result in regards to the research reported in this work as it will also be running IMBH and no IMBH cluster simulations side by side and comparing the results.

2.3 Dragon Simulation

Long Wang et al. modelled four massive GC evolutions, each with 10^6 stars, containing 5% primordial Black Holes, one of the largest N-Body simulations ever [3]. The model ran NBODY6++GPU code, which is specifically designed to be run on a supercomputer for million or more bodies. The code incorporates the effects of dynamic and stellar evolution of each star and the effect of binaries, kicks from Black Holes and a tidal field.

The results show that a subsystem of black holes form at the centre of the GCs causing a core collapse within the first Gyr. Theorists would suggest multiple Black Holes at the core of a GC is not possible as the black holes would begin a violent gravitational dance that would eject all but one (or all) of the Black Holes from the cluster. However, evidence for multiple Black Holes at the centre of GCs comes from Jay Strader et al. at the Very Large Array (VLA) detecting two radio sources at the centre of M22 [1]. The radio luminosity and central location place considerable constraints on their nature, suggesting the most likely explanation is that they are stellar-mass Black Holes.

3 Computational Approach

3.1 Finite Difference Approximation

Since the force on a particle in the cluster depends only on the position ($\ddot{x} = f(x)$), the finite difference method can be used to numerically integrate the position and velocity of the particles with time, and hence advance the evolution of the cluster. This process is named the leapfrog approximation, as the position and velocity are stepped along half a time step out of phase as can be seen in Eqn.7 and Eqn.8. To advance the cluster evolution along, timesteps of dt are used. To get the position and velocity of the particles to the n^{th} timestep, $t = t_0 + ndt$, where t_0 is the initial time, the force is calculated on the i^{th} particle from every other particle (Eqn.1). Therefore, given an initial velocity $\mathbf{v}_i^{-\frac{1}{2}}$, we can calculate the velocity for the next step along $\mathbf{v}_i^{\frac{1}{2}}$ and so on, to the n^{th} step (Eqn.7)

$$\mathbf{v}_i^{n+\frac{1}{2}} = \mathbf{v}_i^{n-\frac{1}{2}} + \frac{\mathbf{F}_i}{m_i} dt. \tag{7}$$

Furthermore, now the velocity is known for each step and, given an initial position $\mathbf{x}_i^0$, the position at any step can be calculated (Eqn.8)

$$\mathbf{x}_i^{n+1} = \mathbf{x}_i^n + \mathbf{v}_i^{n+\frac{1}{2}} dt. \tag{8}$$

The leapfrog approximation is beneficial in this situation as it computes the motion of the particles with great simplicity and with second order accuracy. It stores very few variables, so takes up little space, therefore does not take up much computer memory. This means it can be run for simulations with a large number of particles. An example of this method's utility is for dark matter formation in the universe for billions of particles. Since this method calculates the force from every particle on each particle, the computational load grows proportional to N^2, with N as the total number of particles. This is significant as it limits the size of the clusters this research can investigate.

3.2 N-Body Code

This section details the method followed to generate the data for the GCs with and without IMBHs. First, the initial conditions of the cluster are set up; the initial number of stars was set to N to 400. The initial size of the cluster was set to $R = 1$ and 10 parsecs (3.26 to 32.6 light-years) for four different clusters, with stars being assigned random positions within a sphere (radius R). Star masses were randomly assigned. On average star masses were $M_s = 5M_\odot$, meaning the overall cluster mass of $M_{GC} \approx 2000\ M_\odot$ (without an IMBH). The IMBHs were placed at the centre of the cluster with mass M_{IMBH}=1000 $M_\odot$. Using the cluster densities, the timescale was calculated for a cluster collapse using Eqn.6. The crossing time means that the timestep dt could be calculated ($dt = t_{cr}/nsteps$, where $nsteps$ is the number of steps the leapfrog runs for). All of the initial velocities were set to zero.

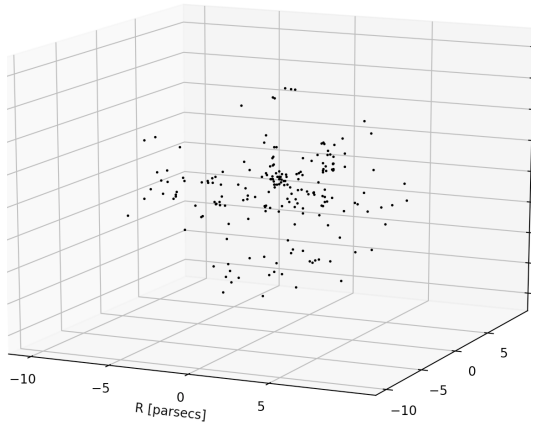

Figure 2. A visual depiction of the research. The initial conditions can clearly be seen; cluster of size $N = 200$ particles, no IMBH present. Particles placed inside sphere $R = 10$ parsecs. Total cluster mass, $M_{TOT} \approx 300M_\odot$ and cluster age is 5 million years old, hence slightly denser core can be seen where collapse is occurring most rapidly.

Secondly, a cluster with R=1 parsec, containing five stellar mass black holes mass M=20 M_{SMBH}, was investigated. The number of stars was set to N=200. The initial positions of stars and Black Holes were randomly assigned, as described before. Black Holes were not allowed to merge as the investigation was to see if any were ejected from the core, using the same code as for one big IMBH.

These initial conditions were run through a position and velocity updater, that used the leapfrog approximation. When particles come close together a very small timestep would be required to deal with the massive accelerations, otherwise the particles will receive massive accelerations and not be decelerated as they move away from close interactions as the leapfrog method will jump them to a distance where the gravitational force is much lower. Therefore, a softening term was introduced into Eqn.1 to make the particles behave, effectively, like balls of radii $\epsilon/2$, where ϵ is the softening constant. This is shown in Eqn.9:

$$\mathbf{F}_i = -G \sum^{N} m_i m_j \frac{\mathbf{r}_i - \mathbf{r}_j}{\left[|r_i - r_j|^2 + \epsilon^2\right]^{\frac{3}{2}}}. \tag{9}$$

The softening constant was set to 0.1R for all simulations. The positions and velocities for each timestep were stored. Using the velocities and positions stored

and Eqn.3 and Eqn.4 the total kinetic and potential energy at every timestep was calculated and plotted against the cluster age. Furthermore, a velocity dispersion profile was calculated as the cluster reached a "steady" state (initial collapse oscillations had calmed down, and kinetic and potential roughly constant). The radial velocity components were recorded and hence velocity dispersion, using $3\sigma_{3D}^2 = v^2$ for each of the particles in the cluster. The radius for each of was recorded for all particles in the cluster. The data was "binned" (arranged into intervals and averaged) and a polynomial curve fit, order 4, using a least squares optimising function in the code.

4 Results and Discussion

The results presented in Fig.3 to Fig.7 follow the collapse of four different clusters, referred to as CG_{BH1}, CG_2, CG_{BH3} and CG_4; where the subscript $_{BH}$ refers to a cluster containing an IMBH (see Fig.3 and Fig.6). They are compared to investigate the effects an IMBH has on the total kinetic and potential energy, and on the velocity dispersion profiles of the different sized clusters (two different sizes; $R = 10$ parsecs and $R = 1$ parsec). A plot or the root mean square velocity and root mean square radius was added for cluster of size $R = 1$ parsec, so key features of the kinetic and potential plot could be compared at certain positional features in the evolution.

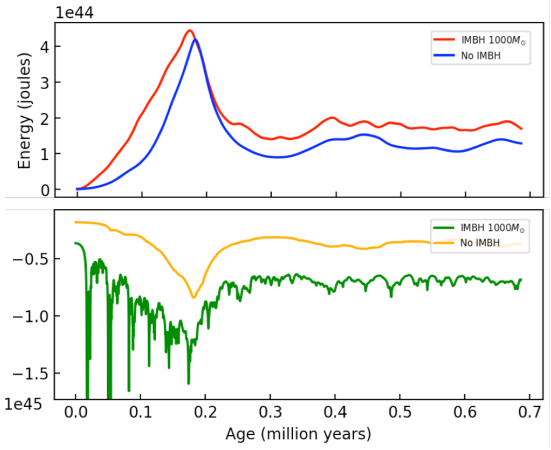

Figure 3. The kinetic and potential energy against the age of the cluster for a simulation with an IMBH, CG_{BH1} (red and green) and without an IMBH, CG_2 (blue and yellow). Both of the clusters have properties: R = 1 parsec, N = 400.

Fig.3 shows that, initially, the kinetic energy for clusters CG_{BH1} and CG_2 both start at zero and rapidly increase. The kinetic energy reaches its maximum value for CG_{BH1} just before CG_2 reaches its maximum of $3.5 \cdot 10^{44}$J and $4.45 \cdot 10^{44}$J at 0.17 and 0.18 million years respectively. The potential energy initially falls for both clusters and reaches a minimum as the kinetic energy peaks. This result is as expected because all of the potential of the cluster has been converted into kinetic energy as the cluster collapses and particles fall towards the core. The total kinetic and the total potential energy both level-off as the cluster stabilises. However, if time averaged values are taken for the stable portion of the clusters evolution (0.3 million years onwards); the simulation reports $2T + V = -1.41 \cdot 10^{44}$ for CG_{BH1} and $2T + V = -1.39 \cdot 10^{44}$ for CG_2. This shows the Virial Theorem, $2T + V = 0$ doesn't hold for either cluster simulation. A hypothetical explanation for this might be that after the initial collapse many particles gained enough velocity to escape the cluster. This means the cluster is no longer made up of particles orbiting a dense core so is not actually stable, with the high kinetic energy of escape particles disturbing the cluster. A solution might be to follow the energy evolution of half-mass radius of the cluster (the radius from the core that contains half the total mass of the cluster) where the particles are probably still contained within the core. However, another possible explanation might be the softening constant is damping particle motions as they have close encounter interactions (the softening constant reduces the force the particles experience in the core). Future solutions may include using a much smaller timestep and reducing the softening constant.

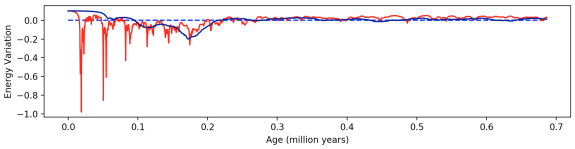

Figure 4. The variation of the total energy of the CG_{BH1} (solid blue line) and CG2 (solid red line) from the time averaged total energy centred on zero (plotted with a blue dashed line) plotted against the age of the cluster. The energy variation had no units as it has been normalised.

The energy variation, Fig. 4, of the total energy from the time averaged energy shows the simulations are not totally conserving energy, especially at early ages where the total energy varies up to 20% from the time averaged total energy (spikes not included). Furthermore, the spikes in energy variation for CG_{BH1} align with the spike in potential in Fig.3. These spikes are not present in CG_2, indicating the IMBH is causing massive jumps in potential energy. This may be a failure of the softening constant to completely eliminate close interactions between particles in the core and the IMBH. Further work may investigate the use of variable timesteps that become much smaller for particles that are close together, to try and eliminate the spikes and reducing the error caused by the finite difference method.

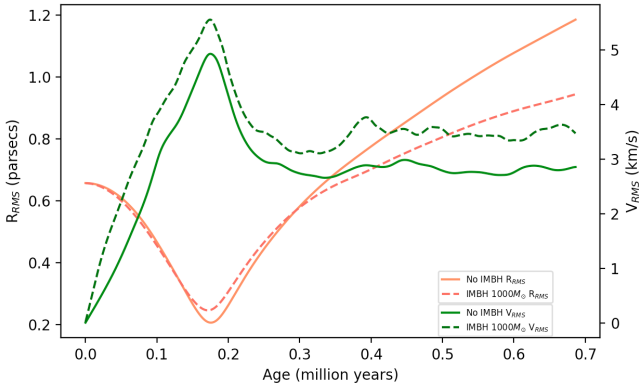

Figure 5. The root mean square velocity, V_{RMS}, plotted against the right hand side axis and root mean square radius, R_{RMS} against the left had side axis, for clusters CG_{BH1}

and CG_2.

The cluster collapse can clearly be seen in Fig.5, as the R_{RMS} reaches a minimum of 0.25 parsecs and 0.21 parsecs for CG_{BH1} and CG_2 respectively. Both cores minimum radii correspond to the maximum kinetic energy and minimum potential energy. The particles have fallen to the bottom of the potential well, nearest the core centre, but have the highest velocities. An interesting result visible in Fig.5 is that the V_{RMS} peaks higher for CG_{BH1}, but CG_2's core shrinks to a smaller size. The particles fall a smaller distance towards the core with an IMBH inside, before the collapse is stabilised. As can be seen in Fig.3 and Fig.5, after the initial collapse at both cores radii increase smoothly outward, but CG_{BH1} expands at a slower rate. A possible explanation is that the IMBH pulls the particles back towards the core.

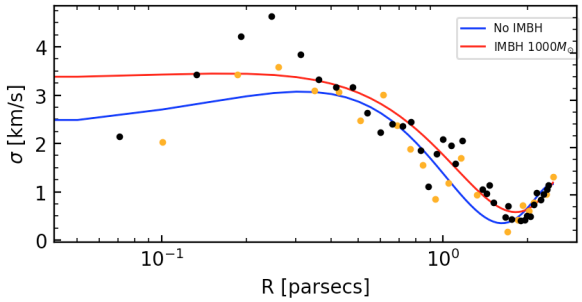

Figure 6. Velocity dispersion profile of clusters CG_{BH1} and CG_2. The black data points correspond to radial velocity measurements from CG_{BH1} and the yellow CG_2 at cluster age 0.7 million years. The data points are fitted with a polynomial, order 4.

The data from Fig.6 shows the velocity dispersion profile is flat near the core, but when moving to the outer reaches of the cluster it decreases, as expected (Eqn.5). The velocity dispersion profile is higher for CG_{BH1} than for CG_2. If the simulation had been set up with the same initial conditions that corresponded to a cluster in the night sky, observed measurements for the radial velocities could be fitted to the profile. A comparison of the observed data to the two simulated clusters could be made to see which was the better fit and hence establish whether or not an IMBH was at the core. To test the accuracy of the profile fitted, a viral mass of $2302M_\odot$ was calculated using Eqn.5 and data points corresponding to the cluster with no IMBH from Fig.6. This gives a fractional error on the total mass of the cluster (M_{TOT}) 15%. A point for future work would be investigating simulations with much higher particle numbers to try and increase the number of data point plotted on the velocity dispersion profile and hence obtain a better fitting polynomial. This could be achieved by running the same code through a supercomputer, or by using methods such as the changing the timing to calculate the force, from particle to particle, depending on the timescale of force variation. This means for interactions at a short range a small timestep is used, but for larger scales, a lower time step is used. More advancements might call for adaptive mesh refinement [6].

The next two simulated clusters were CG_{BH3} and CG_4 shown in Fig.7, with initial cluster radius, $R = 10$ parsecs, N=400 and evolution age equal to the crossing time. This new cluster size dramatically decreased the initial density of the cluster meaning a much longer crossing time for particles and hence a longer collapse time.

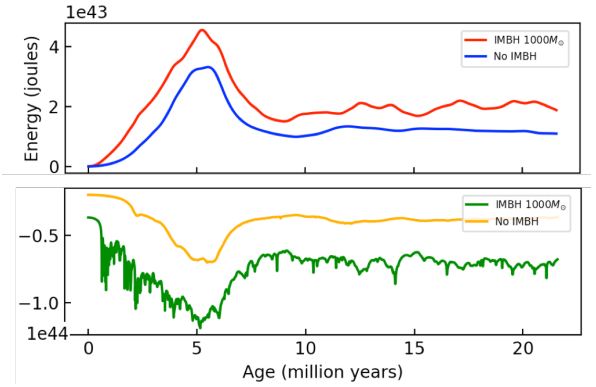

Figure 7. Kinetic and Potential energy vs time for a clusters CG_{BH3}, CG_4.

By comparing Fig.3 and Fig.7 it is clear that a much lower initial concentration reduces the total kinetic energy of both clusters by a factor of ten. This may be because the cluster collapses in stages, with the particles closer in falling towards the centre more rapidly than the stars further out which are experiencing weaker gravitational forces. Therefore, as the outer particles start to pick up speed as they move towards the core, the particles that were closer in have reached their maximum kinetic energy and are starting to move away from the core, and their potential energy is now increasing. This causes the maximum kinetic energy reached to be lower, as particles aren't peaking at the same point in the evolution of the cluster. Furthermore, the width of the peak for both clusters is more spread-out compared with CG_{BH1} and CG_2, showing a collapse over a longer period of time, relative to the age both clusters reach within the simulation limits (defined by the crossing time). However, the overall evolution of the clusters is the same as for CG_{BH1} and CG_2. They exhibit the same key features: the kinetic and potential energy reach a maximum and minimum respectively, as these larger clusters still show an overall collapse and then stabilise fairly afterwards.

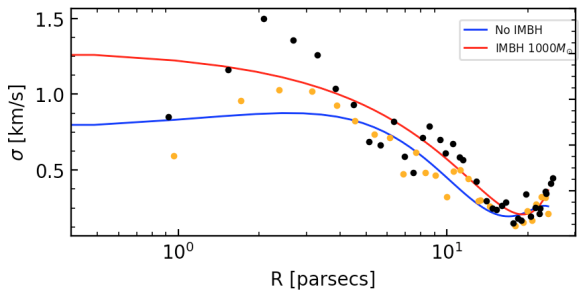

Figure 8. Velocity dispersion profile of cluster simulations CG_{BH3} and CG_4. The profiles axes are ρ_D the velocity dispersion, against, R the radius of the particle in the cluster. The x axis is logarithmic scale.

The velocity dispersion profiles for CG_{BH3} and CG_4 are similar to the previous clusters, however the profile is

flat at a much lower velocity dispersion. Furthermore, both profiles extend over a larger radius. This causes the speeds the particles can reach to be much smaller than for the quicker, more dense, collapse of CG_{BH1} and CG_2.

As a small extension the collapse of a cluster, CG_5 containing five stellar mass Black Holes was followed to investigate whether or not Black Holes are ejected from the core. The cluster had properties N=200, R=1 parsec, and the cluster was allowed to evolve for twenty times longer than the crossing time, to give the Black Holes a greater chance of being ejected. This is a direct comparison to the result found by Long Wang et al. but for a much smaller and simpler model. The simulation for CG_5 showed that the particles were all contained in a tight core with $r < 0.1$ parsecs for all five Black Holes. This seemingly verifies the findings of Long Wang et al. and Jay Strader et al., however it is possible that the softening constant reduced the gravitational force the stellar black holes could exert on each other, therefore they remained in the core rolling around each other.

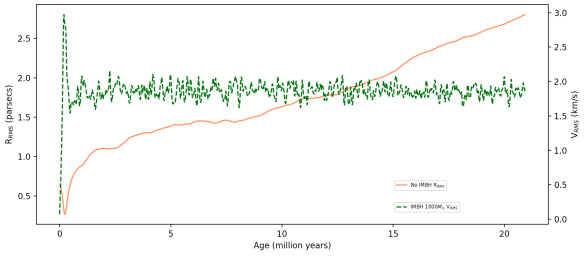

Figure 9. The root mean square velocity, V_{RMS}, plotted against the right hand side axis and root mean square radius, R_{RMS} against the left had side axis, for cluster CG_5. The simulation was allowed to run for $20 \cdot t_{cr}$

The root mean square radius of the cluster initially decreased for the collapse and then slowly increased, with no levelling-off, seen in Fig.9. This may be due to the initial particles that escaped from the cluster that kept moving away. Again, a half-mass radius calculation may be needed to investigate the motion of particles that remained bound to the cluster. An interesting point from Fig.9 is the root mean square velocity. After the collapse, the V_{RMS} jumps around between 1.5km/s and 2km/s. This corresponds to particles in the core falling towards the Black Holes and away from them again. It shows the core is still very active whilst the particles that have escaped move away with at relatively constant speed, that could

5 Conclusion

In conclusion, the simulations for all clusters show clear collapse, with kinetic and potential energy stabilising quickly after collapse. The results show the Virial Theorem doesn't hold for any of the simulations. This may be due to the softening constant removing energy from the system, or maybe due to expelled particles that are no longer part of the cluster. This leads onto the fact that energy isn't conserved, with up to 20% variation from what we would expect during the core collapse (not including spikes). A lower initial density of the cluster caused the maximum kinetic and minimum potential energy to be lower, as the cluster collapsed more slowly, with in outer most particles taking longer to reach their maximum kinetic energy. The velocity dispersion profiles are larger for clusters containing IMBHs, therefore simulations like this one could be used to test for the presence of IMBHs against observed data from real GCs. Velocity dispersion profiles for the cores at later stages of their evolution were also found to be much lower for the cores that were less dense initially. It was also found for the simulations that the cluster contain 5 stellar mass black holes, none were ejected.

Some limitations in the code such as the need for a softening constant in the force equation to prevent the leapfrog approximation overstepping the particles may be responsible for errors in energy conservation and not confirming the virial theorem. For future work smaller time steps are needed in the core which would allow a smaller softening constant to be used. Furthermore, varying the timestep so that closer interactions had shorted steps would improve the accuracy of this work.

References

[1] Jay Strader et al. (2012). Two stellar-mass black holes in the globular cluster M22. Published by Nature Publishing Group, Volume 490.

[2] Dr H Baumgardt et al. (2016). N-body modeling of globular clusters: Masses, mass-to-light ratios and intermediate-mass black holes. Published in Monthly Notices of the Royal Astronomical Society, Volume 464, Issue 2.

[3] Long Wang et al (2016). The DRAGON simulations: globular cluster evolution with a million stars. Publication in Monthly Notices of the Royal Astronomical Society, Volume 458, Issue 2.

[4] Irvin Isenberg (1950). The Virial Theorem and Variational Principles. University of Chicago.

[5] Florent Renaud et al. (2016). The origin of the Milky Way globular clusters. Publication in Monthly Notices of the Royal Astronomical Society, Volume 465, Issue 3.

[6] Hideki Yahagi et al. (2001). N-Body code with adaptive mesh refinement. Published in The Astrophysical Journal, volume 558.

[7] Aarseth S. J., Lin D. N. C., Papaloizou J. C. B. (1988) On the collapse and violent relaxation of protoglobular clusters. Astrophys. J. 324:288–310,